Since January 2020 Elsevier has created a COVID-19 resource centre with free information in English and Mandarin on the novel coronavirus COVID-19. The COVID-19 resource centre is hosted on Elsevier Connect, the company's public news and information website.

Elsevier hereby grants permission to make all its COVID-19-related research that is available on the COVID-19 resource centre - including this research content - immediately available in PubMed Central and other publicly funded repositories, such as the WHO COVID database with rights for unrestricted research re-use and analyses in any form or by any means with acknowledgement of the original source. These permissions are granted for free by Elsevier for as long as the COVID-19 resource centre remains active.

Epidemics 42 (2023) 100664

Contents lists available at ScienceDirect

Epidemics

journal homepage: www.elsevier.com/locate/epidemics

How time-scale differences in asymptomatic and symptomatic transmission shape SARS-CoV-2 outbreak dynamics

Jeremy D. Harris [a,*,1], Sang Woo Park [b,*,1], Jonathan Dushoff [c,d,e,*], Joshua S. Weitz [a,f,g,*]

[a] School of Biological Sciences, Georgia Institute of Technology, Atlanta, GA, USA
[b] Department of Ecology and Evolutionary Biology, Princeton, NJ, USA
[c] Department of Biology, McMaster University, Hamilton, Ontario, Canada
[d] Department of Mathematics and Statistics, McMaster University, Hamilton, Ontario, Canada
[e] M. G. DeGroote Institute for Infectious Disease Research, McMaster University, Hamilton, Ontario, Canada
[f] School of Physics, Georgia Institute of Technology, Atlanta, GA, USA
[g] Institut de Biologie, École Normale Supérieure, Paris, France

ARTICLE INFO

Dataset link: https://doi.org/10.5281/zenodo.7523452

Keywords:
SARS-COV-2
COVID-19
Asymptomatic transmission
Epidemic dynamics

ABSTRACT

Asymptomatic and symptomatic SARS-CoV-2 infections can have different characteristic time scales of transmission. These time-scale differences can shape outbreak dynamics as well as bias population-level estimates of epidemic strength, speed, and controllability. For example, prior work focusing on the initial exponential growth phase of an outbreak found that larger time scales for asymptomatic vs. symptomatic transmission can lead to under-estimates of the basic reproduction number as inferred from epidemic case data. Building upon this work, we use a series of nonlinear epidemic models to explore how differences in asymptomatic and symptomatic transmission time scales can lead to changes in the realized proportion of asymptomatic transmission throughout an epidemic. First, we find that when asymptomatic transmission time scales are longer than symptomatic transmission time scales, then the effective proportion of asymptomatic transmission increases as total incidence decreases. Moreover, these time-scale-driven impacts on epidemic dynamics are enhanced when infection status is correlated between infector and infectee pairs (e.g., due to dose-dependent impacts on symptoms). Next we apply these findings to understand the impact of time-scale differences on populations with age-dependent assortative mixing and in which the probability of having a symptomatic infection increases with age. We show that if asymptomatic generation intervals are longer than corresponding symptomatic generation intervals, then correlations between age and symptoms lead to a decrease in the age of infection during periods of epidemic decline (whether due to susceptible depletion or intervention). Altogether, these results demonstrate the need to explore the role of time-scale differences in transmission dynamics alongside behavioral changes to explain outbreak features both at early stages (e.g., in estimating the basic reproduction number) and throughout an epidemic (e.g., in connecting shifts in the age of infection to periods of changing incidence).

1. Introduction

The role of asymptomatic carriers in driving epidemic dynamics has remained a key question throughout the SARS-CoV-2 pandemic (Chan et al., 2020; Pan et al., 2020; Johansson et al., 2021; Bai et al., 2020). Asymptomatic carriers have reduced the effectiveness of non-pharmaceutical interventions (Fraser et al., 2004; Brett and Rohani, 2020; Chinazzi et al., 2020; Wu et al., 2020; Johansson et al., 2021; Kinoshita et al., 2020), and have made it more difficult to obtain unbiased estimates of disease severity, including infection fatality ratios (Russell et al., 2020). Although several studies have estimated the prevalence of asymptomatic SARS-CoV-2 infections in various settings (Nishiura et al., 2020; Mizumoto et al., 2020; Oran and Topol, 2020; Lee et al., 2020; Long et al., 2020), there is still considerable uncertainty in how the transmission dynamics of asymptomatic individuals differ from those of symptomatic individuals. Modeling studies have typically assumed that asymptomatic and symptomatic individuals are infected for an equal amount of time. Some studies have further accounted for the possibility that asymptomatic individuals may transmit

* Corresponding authors.
E-mail addresses: jeremy.harris@gatech.edu (J.D. Harris), swp2@princeton.edu (S.W. Park), dushoff@mcmaster.ca (J. Dushoff), jsweitz@gatech.edu (J.S. Weitz).
[1] These authors contributed equally.

https://doi.org/10.1016/j.epidem.2022.100664
Received 28 June 2022; Received in revised form 7 December 2022; Accepted 24 December 2022
Available online 10 January 2023
1755-4365/© 2023 The Author(s). Published by Elsevier B.V. This is an open access article under the CC BY license (http://creativecommons.org/licenses/by/4.0/).

less than symptomatic individuals, but the range of assumptions vary widely (from 90% less transmissible (Ferretti et al., 2020) to equally transmissible (Lavezzo et al., 2020)).

Prior work has shown that individual-level differences in transmission time scales between asymptomatic and symptomatic transmission can have important implications for estimates of epidemic dynamics during the exponential growth phase (Park et al., 2020). For example, if asymptomatic individuals are able to transmit for a longer period of time than symptomatic individuals, the proportion of new infections attributable to asymptomatic transmission will be lower than predicted based on their intrinsic infectiousness because shorter transmission intervals drive the spread during the epidemic growth phase. Under the same scenario, failing to account for differences in time scales of asymptomatic and symptomatic transmission can lead to underestimation of the basic reproduction number (i.e., the average number of secondary infections caused by a primary case (Anderson and May, 1992; Diekmann and Heesterbeek, 2000; Diekmann et al., 1990; Van den Driessche and Watmough, 2002)) from the epidemic growth rate (Park et al., 2020).

These differences in transmission time scales may result from a combination of biological and behavioral factors. For example, individuals who have higher viral load are more likely to develop symptoms (Marks et al., 2021; Zheng et al., 2020) and have shorter incubation periods (Jones et al., 2021; Marks et al., 2021; Ke et al., 2020), which in turn can lead to earlier onset of infectiousness. Symptomatic individuals may also self-isolate after the onset of symptoms, thereby preventing symptomatic transmission later in the infection (He et al., 2020). Intervention measures that target symptomatic individuals can further bias transmission toward early in the infection. Taken together, behavioral and biological factors may effectively cause symptomatic individuals to transmit for a shorter period of time.

The impact of transmission time-scale differences on epidemic inference can be approached using a generation interval-based framework (Heesterbeek and Dietz, 1996). The generation interval, defined as the time between when an individual is infected and when that individual transmits to another person, connects individual-level transmission time scales with population-level measures of disease spread (Wallinga and Lipsitch, 2007; Wallinga and Teunis, 2004; Svensson, 2007; Champredon and Dushoff, 2015). For example, given an observed epidemic growth rate, a disease with longer generation intervals on average will be associated with a higher reproduction number (Park et al., 2019). This result applies here: if asymptomatic cases have longer generation intervals the overall average generation interval is increased (Park et al., 2020).

Symptomaticity of infections may also correlate with transmission outcomes. That is, new infections caused by asymptomatic transmission may be more likely to remain asymptomatic than new infections caused by symptomatic individuals, leading to correlations between disease statuses of the infector and of the infectee (Wu et al., 2020). Such correlations might arise from dose-dependent responses: recent animal-model studies have shown such responses to COVID-19 infection, with higher initial viral inoculum associated with both increased viral shedding and more severe outcomes (Ryan et al., 2021; Imai et al., 2020); data from animal model studies of other human coronaviruses, including SARS-CoV, have shown similar trends (Watanabe et al., 2010). If symptomatic infections typically shed more infectious virus than asymptomatic infections, then the initial viral dose from symptomatic transmission would be higher on average than from asymptomatic transmission, making symptomatic infections more likely, and generating correlations between disease statuses of the infector and the infectee.

Correlations might also arise from age-dependent assortativity in mixing patterns and variation in symptomaticity. Higher contact rates among individuals of similar ages (e.g., in schools) cause more transmission within similar age groups (as opposed to between different age groups). As disease symptomaticity of SARS-CoV-2 varies with age (Davies et al., 2020; Wu et al., 2020), disease statuses of infectees may effectively correlate with disease statuses of their infectors. Irrespective of the mechanism, we predict that such correlations can have important dynamical consequences when they are coupled with the effects of differences in time scales of transmission: if the proportion of new infections attributable to asymptomatic transmission changes over the course of an epidemic, these correlations may amplify changes in the realized proportion of asymptomatic incidence.

In this study, we examine the impacts of individual-level differences between asymptomatic and symptomatic transmission on population-level disease dynamics. First, we consider the possibility that asymptomatic individuals may transmit more slowly (i.e., have longer generation intervals on average) than symptomatic individuals. We show that such slow transmission by asymptomatic individuals would increase the realized proportion of asymptomatic transmission during periods when total transmission is declining—a robust pattern whether the decline is driven by susceptible depletion or by changes in effective contacts. Second, we account for the correlations between transmission outcomes and individual disease statuses. In this case, we find that the proportion of asymptomatic transmission as well as a new effect: the proportion of asymptomatic *incidence* can also increase as the epidemic declines.

Finally, we study the dynamics of an age-dependent model that includes assortative mixing and a greater proportion of asymptomatic infections in younger than older individuals. In this example, the average age of an incident infection increases as the epidemic progresses, because of faster depletion of susceptibles in younger age classes. Because the probability of symptomatic infections increases with age, this leads to changes in the realized proportion of asymptomatic transmission and incidence. In an intervention scenario, the average age of an incident infection remains nearly constant when asymptomatic and symptomatic generation-interval distributions are identical. However, when asymptomatic generation intervals are longer, the average age of an incident infection decreases as the epidemic decays, causing the realized proportion of asymptomatic incidence to increase. Together, these analyses demonstrate the potential for individual-level variation in transmission dynamics to shape the realized proportion of asymptomatic transmission and incidence throughout an epidemic.

2. Methods

2.1. SEIR model of asymptomatic transmission with a fixed intrinsic proportion of asymptomatic incidence

We study the impact of differences in asymptomatic and symptomatic generation-interval distributions on epidemic dynamics using a series of Susceptible–Exposed–Infectious–Recovered (SEIR) models. Once infected, susceptible individuals enter an exposed but latent stage, during which they cannot transmit. The first model assumes that a fixed proportion p – which we refer to as the intrinsic proportion of asymptomatic infections – of newly infected individuals remains asymptomatic over the course of infection while transmitting at rate β_a. The remaining proportion $1-p$ develops symptoms after the exposed period and transmit at rate β_s. Then, the proportion of individuals in each compartment can be described by the following set of equations:

$$\begin{aligned}
\dot{S} &= -\left(\lambda_a(t)+\lambda_s(t)\right) S \\
\dot{E}_a &= p\left(\lambda_a(t)+\lambda_s(t)\right) S - E_a/\tau \\
\dot{E}_s &= (1-p)\left(\lambda_a(t)+\lambda_s(t)\right) S - E_s/\tau \\
\dot{I}_a &= E_a/\tau - I_a/T_a \\
\dot{I}_s &= E_s/\tau - I_s/T_s \\
\dot{R} &= I_a/T_a + I_s/T_s \ , \qquad (1)
\end{aligned}$$

where subscripts denote asymptomatic (a) vs. symptomatic (s) classes. Here,

$$\lambda_a(t) = \beta_a I_a \ , \ \lambda_s(t) = \beta_s I_s$$

denote the forces of infection caused by asymptomatic and symptomatic individuals, respectively, $1/\tau$ is the mean exposed period, and T_a (T_s) is the mean duration of asymptomatic (symptomatic) infectious periods. Since infectious period is assumed to be exponentially distributed, the mean generation interval is equal to the sum of the mean exposed and infectious periods (Svensson, 2007; Wallinga and Lipsitch, 2007; Roberts and Heesterbeek, 2007).

For this model, the subgroup reproduction number of asymptomatic (symptomatic) individuals is given by $\mathcal{R}_{0,a} = \beta_a T_a$ ($\mathcal{R}_{0,s} = \beta_s T_s$) and defined as the number of secondary infections caused by a single asymptomatically (symptomatically) infected individual in a fully susceptible population. The basic reproduction number of the system is the weighted average of the two subgroup reproduction numbers:

$$\mathcal{R}_0 = p\,\mathcal{R}_{0,a} + (1-p)\,\mathcal{R}_{0,s}. \tag{2}$$

Then, we can define the intrinsic proportion of asymptomatic transmission, which represents the relative contribution of asymptomatic transmission towards the basic reproduction number (Park et al., 2020):

$$z = \frac{p\,\mathcal{R}_{0,a}}{p\,\mathcal{R}_{0,a} + (1-p)\,\mathcal{R}_{0,s}}. \tag{3}$$

We also define the realized proportion of asymptomatic transmission, $q(t)$, the proportion of new infections caused by asymptomatically infected individuals at time t:

$$q(t) = \frac{\lambda_a(t)}{\lambda_a(t) + \lambda_s(t)}\ . \tag{4}$$

If asymptomatic and symptomatic individuals have identical generation-interval distributions, then $q(t) = z$. However, if the generation-interval distributions differ, then the realized proportion of asymptomatic transmission can systematically differ from the intrinsic proportion of asymptomatic transmission, not only during exponential growth but also as the epidemic progresses.

Here, we generalize prior work (Park et al., 2020), which focused on the initial exponential growth phase, and we explore how the realized proportion of asymptomatic transmission changes over the course of an epidemic when we assume that asymptomatic infections have longer infectious periods (and therefore longer generation intervals). To do so, we assume the mean exposed period is $\tau = 3$ days for both groups and fix the mean infectious period to $T_s = 5$ days for symptomatic infections. We then explore changes in the mean infectious period between $T_a = 5$ to $T_a = 8$ days for asymptomatic infections. To compare across simulations, we fix the intrinsic proportion of asymptomatic infections ($p = 0.4$). We set the subgroup reproduction numbers are equal, i.e., $\mathcal{R}_{0,a} = \mathcal{R}_{0,s}$, and vary transmission such that the exponential growth rate is matched across simulations ($r = 0.14$/day). We also provide a supplemental figure that shows simulations when transmission rates are equal. We show simulations for both susceptible depletion and intervention scenarios. For intervention, rates of asymptomatic and symptomatic transmission are reduced by an equal factor such that the effective reproduction number is reduced over a period of 30 days starting from 70 days into the simulation. The mitigation intensities are chosen so that the final effective reproduction numbers match those observed in the susceptible depletion scenario for each infectious period. See Table 1 for parameter descriptions and Figure S1 for model schematic in Supplementary material.

2.2. SEIR model of asymptomatic transmission with correlations between transmission outcomes and disease statuses

Next, we introduce correlations between transmission outcomes and disease statuses: that is, transmission from asymptomatic (symptomatic) individuals is more likely to lead to new, asymptomatic (symptomatic) infections. To study the effects of such correlations on epidemic dynamics, we extend the model in Eq. (1):

$$\begin{aligned}
\dot{S} &= -\left(\lambda_a(t) + \lambda_s(t)\right)\ S \\
\dot{E}_a &= \left(p_{a|a}\,\lambda_a(t) + p_{a|s}\,\lambda_s(t)\right)\ S - E_a/\tau \\
\dot{E}_s &= \left((1-p_{a|a})\,\lambda_a(t) + (1-p_{a|s})\,\lambda_s(t)\right)\ S - E_s/\tau \\
\dot{I}_a &= E_a/\tau - I_a/T_a \\
\dot{I}_s &= E_s/\tau - I_s/T_s \\
\dot{R} &= I_a/T_a + I_s/T_s\ .
\end{aligned} \tag{5}$$

Here, $p_{a|a}$ ($p_{a|s}$) is the probability of an asymptomatic infectee given transmission from an asymptomatic (symptomatic) infector, whereas $p_{s|a} = 1 - p_{a|a}$ ($p_{s|s} = 1 - p_{a|s}$) is the probability of a symptomatic infectee given transmission from an asymptomatic (symptomatic) infector. When $p_{a|a} = p_{a|s}$, the model in Eq. (5) reduces to the model in Eq. (1).

The realized proportion of asymptomatic transmission is still given by Eq. (4). The realized proportion of asymptomatic *incidence* needs to account for the new correlations:

$$p(t) = \frac{p_{a|a}\,\lambda_a(t) + p_{a|s}\,\lambda_s(t)}{\lambda_a(t) + \lambda_s(t)}. \tag{6}$$

We explore the effect of correlations between transmission outcomes and disease statuses by letting $p_{a|a} = 0.50$ and $p_{a|s} = 0.25$ (Wu et al., 2020) while holding the exponential growth rate fixed at $r = 0.14$/day across simulations. As before, we assume the subgroup basic reproduction numbers are equal, $\mathcal{R}_{0,s} = \mathcal{R}_{0,a}$, and provide corresponding supplemental figures assuming transmission rates are equal. We also provide a supplemental figure assuming $\mathcal{R}_{0,s} = 4\,\mathcal{R}_{0,a}$ and ranging over the ratio of infectious periods: $T_a/T_s = [5/8, 8/5]$. We do so by fixing $T_a = 5$ days while decreasing T_s from 8 to 5 days and fixing $T_s = 5$ days while increasing T_a from 5 to 8 days. See Table 1 for parameter descriptions and Figure S1 for model schematic in Supplementary material.

2.3. SEIR model of asymptomatic transmission with assortative mixing and variation in the chance of symptomatic infection by age

Finally, we study an age-stratified model as an example of how correlations might arise between transmission outcomes and disease statuses. The model couples age-dependent assortative mixing patterns with variation in the proportion of asymptomatic (vs. symptomatic) outcomes that increase with age. Hence, if younger individuals are more likely to remain asymptomatic and assortatively mix with younger individuals, then asymptomatic infections will effectively cause more asymptomatic infections than symptomatic infections. To examine these potential age-dependent effects, we stratify the population into age groups spanning intervals of 10 years, going from 0–9 ($n = 1$) up to 60–69 ($n = 7$) with the last group being 70+ ($n = 8$). Each age group n consists of 6 compartments (S_n, $E_{n,a}$, $E_{n,s}$, $I_{n,a}$, $I_{n,s}$, and R_n) representing the number of individuals in each disease state such that $S_n + E_{n,a} + E_{n,s} + I_{n,a} + I_{n,s} + R_n = A_n$, where A_n is the population size in age group n.

We model the contact patterns between the age groups by including an empirically estimated contact matrix, $(C_{n,m})_{n,m=1}^{N}$, where $C_{n,m}$ is the average number of contacts (per day) that individuals in age group n make with individuals in age group m (Zhang et al., 2020). In our simulations, we use the baseline contact estimates of Shanghai that were empirically estimated prior to the COVID-19 outbreak, which shows a high degree of age-dependent assortative mixing (Zhang et al., 2020) (see Table S1 in Supplementary material). To be consistent with estimates of contact rates, we let A_n be the age distribution of the population of Shanghai. We vary the proportion of asymptomatic incidence with respect to age, p_n (Davies et al., 2020). In this model, we introduce intervention earlier than in the previous models (50 days into the simulation) to ensure limited susceptible depletion across all of the age groups. We match the exponential growth rate across simulations ($r = 0.14$/day), and assume that $\mathcal{R}_{0,a} = \mathcal{R}_{0,s}$. See Table 1 for parameter descriptions.

Table 1
Parameters, Values, Descriptions. SEIR models with asymptomatic and symptomatic infections. For the base models and the age-dependent model, parameter ranges include both main and supplemental figures. For the base models, given the asymptomatic proportion(s), a single transmission rate is estimated to match the fixed exponential growth rate, r, given asymptomatic and symptomatic infectious periods, T_a and T_s, and assuming one additional constraint: $\mathcal{R}_{0,s} = \mathcal{R}_{0,a}$ (main figures, Figure S2, Figure S8), $\beta_s = \beta_a$ (Figure S3, Figure S6, Figure S9), or $\mathcal{R}_{0,s} = 4\,\mathcal{R}_{0,a}$ (Figure S5, Figure S7). The additional constraint yields the other transmission rate, and the basic reproduction number is calculated from these values. Following the approach in Park et al. (2020), we fix $r = 0.14$ and vary over the ratio of mean asymptomatic vs. symptomatic generation interval. Here, we do so by varying the infectious periods T_a and T_s from 5 to 8 days. See Supplementary material for all supplemental figures.

Base model

Parameter	Value	Description
β_a	0.0959–0.554 days^{-1}	Transmission rate of asymptomatic infections
β_s	0.342–1.08 days^{-1}	Transmission rate of symptomatic infections
T_a	5-8 days (Byrne et al., 2020)	Infectious period of asymptomatic infections, respectively
T_s	5-8 days (Byrne et al., 2020)	Infectious period of symptomatic infections
τ	3 days (Li et al., 2020)	Exposed period or latent stage
r	0.14 days^{-1}	Exponential growth rate
$\mathcal{R}_0$	2.41–2.96	Basic reproduction number
p	0.40 (Lee et al., 2020; Mizumoto et al., 2020)	Proportion of new infections that are asymptomatic
$p_{a\|a}$	0.50 (Wu et al., 2020)	Probability of an asymptomatic infectee given transmission from an asymptomatic infector
$p_{a\|s}$	0.25 (Wu et al., 2020)	Probability of an asymptomatic infectee given transmission from a symptomatic infector

Age-dependent model

Parameter	Value	Description
$\tilde{\beta}_a$	0.0317–0.0445	Age-scaled asymptomatic transmission factor
$\tilde{\beta}_s$	0.0445–0.0508	Age-scaled symptomatic transmission factor
$\mathcal{R}_0$	2.41–2.86	Basic reproduction number
p_n	Fig. 2b in Davies et al. (2020)	Proportion of asymptomatic incidence for age group n
A_n	Table S3 in Zhang et al. (2020)	Population age distribution of Shanghai
$C_{n,m}$	See Table S1 in Supplementary material	Average number of contacts between individuals in age group n with individuals in age group m

Then the number of individuals in each age group and disease state can be described by the following set of equations:

$$\begin{aligned}
\dot{S}_n &= -\left(\lambda_{a,n}(t) + \lambda_{s,n}(t)\right) S_n \\
\dot{E}_{a,n} &= p_n \left(\lambda_{a,n}(t) + \lambda_{s,n}(t)\right) S_n - E_{a,n}/\tau \\
\dot{E}_{s,n} &= (1-p_n) \left(\lambda_{a,n}(t) + \lambda_{s,n}(t)\right) S_n - E_{s,n}/\tau \\
\dot{I}_{a,n} &= E_{a,n}/\tau - I_{a,n}/T_a \\
\dot{I}_{s,n} &= E_{s,n}/\tau - I_{s,n}/T_s \\
\dot{R}_n &= I_{a,n}/T_a + I_{s,n}/T_s \,,
\end{aligned} \tag{7}$$

where the forces of infection for each age group n due to asymptomatic (a) and symptomatic (s) transmission are given by

$$\begin{aligned}
\lambda_{a,n}(t) &= \tilde{\beta}_a \left(\sum_{m=1}^{N} C_{n,m} \frac{I_{a,m}(t)}{A_m} \right), \\
\lambda_{s,n}(t) &= \tilde{\beta}_s \left(\sum_{m=1}^{N} C_{n,m} \frac{I_{s,m}(t)}{A_m} \right).
\end{aligned} \tag{8}$$

As before, we compute the realized proportion of asymptomatic transmission over time

$$q(t) = \frac{\sum_{n=1}^{N} \lambda_{a,n}(t)\, S_n(t)}{\sum_{n=1}^{N} \left(\lambda_{a,n}(t) + \lambda_{s,n}(t)\right) S_n(t)}, \tag{9}$$

as well as the realized proportion of asymptomatic incidence over time,

$$p(t) = \frac{\sum_{n=1}^{N} p_n \left(\lambda_{a,n}(t) + \lambda_{s,n}(t)\right) S_n}{\sum_{n=1}^{N} \left(\lambda_{a,n}(t) + \lambda_{s,n}(t)\right) S_n}. \tag{10}$$

We also calculate the average age of an incident infection over time:

$$\bar{a}(t) = \sum_{n=1}^{N} M_n \left(\frac{i_n(t)}{i(t)} \right), \tag{11}$$

where M_n is the midpoint of age group n, $i_n(t) = \left(\lambda_{a,n}(t) + \lambda_{s,n}(t)\right) S_n$ is the incidence of age group n, and $i(t) = \sum_{n=1}^{N} i_n(t)$ is the total incidence across all age groups.

3. Results

3.1. Effects of differences asymptomatic and symptomatic generation intervals

We first study the effects of differences asymptomatic and symptomatic generation intervals using the SEIR model by fixing intrinsic proportion of asymptomatic incidence, p. To do so, we simulate the model under two scenarios: (1) 'Susceptible Depletion', where the epidemic spreads without mitigation, and (2) 'Intervention', where intrinsic transmission rates of asymptomatic and symptomatic infections are exogenously reduced by the same proportion. Since the exponential growth rate is matched across simulations, the incidence curves start off identically across all simulations (Fig. 1A,E). When the mean infectious period of asymptomatic individuals is longer than that of symptomatic individuals ($T_s = 5$ days), the incidence curves decay more slowly ($T_a = 6$ days, purple and $T_a = 8$ days, light blue). In this case the realized proportion of asymptomatic transmission, $q(t)$, also increases over time because slower generation intervals of asymptomatic individuals become relatively more important during the decay phase (Fig. 1B,F). The differences in the mean infectious periods of asymptomatic and symptomatic individuals do not affect the realized proportion of asymptomatic incidence (Fig. 1C,G). Since changes in the realized proportion of asymptomatic transmission, $q(t)$, are determined by the epidemic growth/decay rate (Park et al., 2020), we are able to match the magnitude of changes in the realized proportion of asymptomatic transmission between susceptible depletion and intervention scenarios by matching their final effective reproduction numbers (Fig. 1B,F).

We further investigate how the magnitude and timing of intervention affect the realized proportion of asymptomatic transmission. When we fix the final effective reproduction and vary the mitigation onset time, the resulting realized proportions of asymptomatic transmission $q(t)$ show similar trajectories and identical asymptotic values across all scenarios because $q(t)$ is determined by the exponential decay rate (Figure S2A-D). When we fix the mitigation onset time and vary the

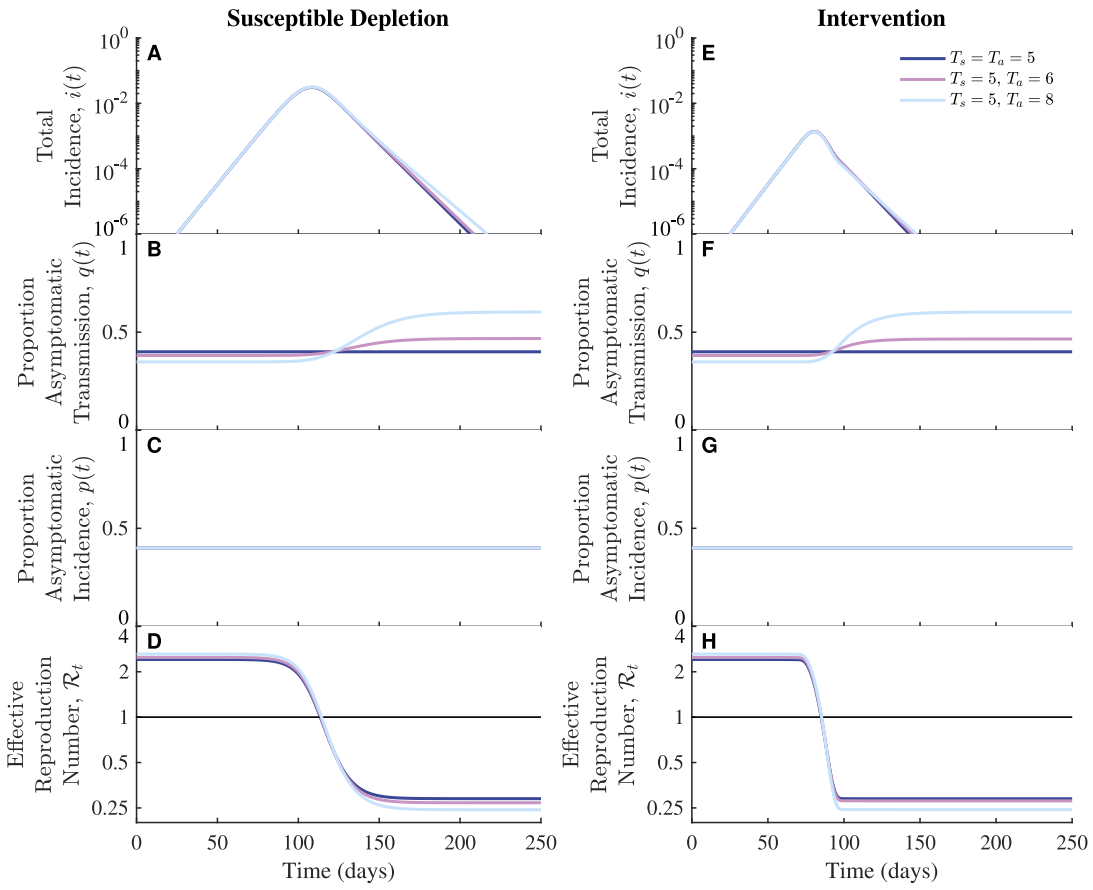

Fig. 1. Effects of differences in asymptomatic and symptomatic generation-interval distributions on the population-level dynamics of asymptomatic infections. We fix the infectious period of symptomatic infections, $T_s = 5$ days and increase the infectious period of asymptomatic infections from $T_a = 5$ days (dark blue), $T_a = 6$ days (purple), $T_a = 8$ days (light blue). (A–D) Without intervention the epidemic spreads through the susceptible population unhindered. As total incidence decreases, the proportion of asymptomatic transmission increases over time when asymptomatic infectious periods are longer than symptomatic infectious periods (purple and light blue). (E–H) With intervention, the reproduction number is reduced over a period of 30 days with mitigation intensities such that the final effective reproduction numbers match those in the susceptible depletion case. Across all simulations, the intrinsic proportion of asymptomatic incidence is $p = 0.40$, and the exponential growth rate is $r = 0.14$/day (Methods). Other parameter values: $\mathcal{R}_0 = 2.41$, $\beta_a = \beta_s = 0.483$ days^{-1} (dark blue); $\mathcal{R}_0 = 2.49$, $\beta_a = 0.415$ days^{-1}, $\beta_s = 0.498$ days^{-1} (purple); $\mathcal{R}_0 = 2.62$, $\beta_a = 0.328$ days^{-1}, $\beta_s = 0.524$ days^{-1} (light blue).

final effective reproduction number, more intense interventions cause incidence to decay faster, which in turn corresponds to a larger increase in the realized proportion of asymptomatic transmission (Figure S2E–G).

We obtain similar results when we assume the transmission rates are equal for asymptomatic and symptomatic infections (Figure S3), rather than assuming the reproduction numbers are equal (as in Fig. 1). The magnitude of changes in the proportion of asymptomatic transmission are similar across both cases (equal transmission rates vs. equal basic reproduction numbers). The one difference is in the initial realized proportion of asymptomatic transmission. When the reproduction numbers are equal, the initial realized proportion of asymptomatic transmission is lower than the intrinsic proportion of asymptomatic incidence (Fig. 1B,F), whereas when transmission rates are equal, the initial realized proportion of asymptomatic transmission is greater than the intrinsic proportion of asymptomatic incidence (Figure S3B,F).

The risk of transmission from contact with asymptomatic individuals may be less than from symptomatic individuals (Buitrago-Garcia et al., 2020; Wu et al., 2020). A recent study used viral load kinetics (in patients with known disease statuses) to estimate the risk of transmission from symptomatic cases to be about 4 times that of asymptomatic cases (odds ratio, 3.79; 95% confidence interval, 2.06–6.95; Wu et al., 2020). Thus, we also examine the effects on the realized proportion of asymptomatic transmission as the ratio of reproduction numbers, $\mathcal{R}_{0,s}/\mathcal{R}_{0,a}$, is increased from one up to four. For a given set of time scales, the discrepancy between the realized proportion of asymptomatic transmission and the intrinsic proportion of asymptomatic transmission is reduced with increased reproduction number ratio, $\mathcal{R}_{0,s}/\mathcal{R}_{0,a}$ (Figure S4A). In addition, increases in the realized proportion of asymptomatic transmission over time are smaller for larger reproduction number ratios (Figure S4B). The qualitative effects of differences between asymptomatic and symptomatic infectious periods on the realized proportion of asymptomatic transmission are similar to each other but reduced in magnitude (Figure S5).

3.2. Effects of correlations between transmission outcomes and disease statuses

Next, we study the effects of correlations between transmission outcomes and disease statuses of the infectors on epidemic dynamics across two scenarios (with and without intervention). A recent study found that approximately 50% of cases likely caused by close contact with asymptomatic index cases were asymptomatic infections and approximately 25% of cases likely caused by close contact with symptomatic index cases were asymptomatic infections (Wu et al., 2020). Hence, we let $p_{a|a} = 0.50$ and $p_{a|s} = 0.25$ and match the exponential growth rate across simulations (Methods). When the mean infectious periods of asymptomatic and symptomatic infections are equal, correlations between transmission outcomes and disease statuses have no effect on epidemic dynamics: the incidence curves (Fig. 2A,E; dashed dark blue) are identical to those in the case with fixed intrinsic proportion asymptomatic incidence (indicated by '$p = 0.40$'). The realized proportions

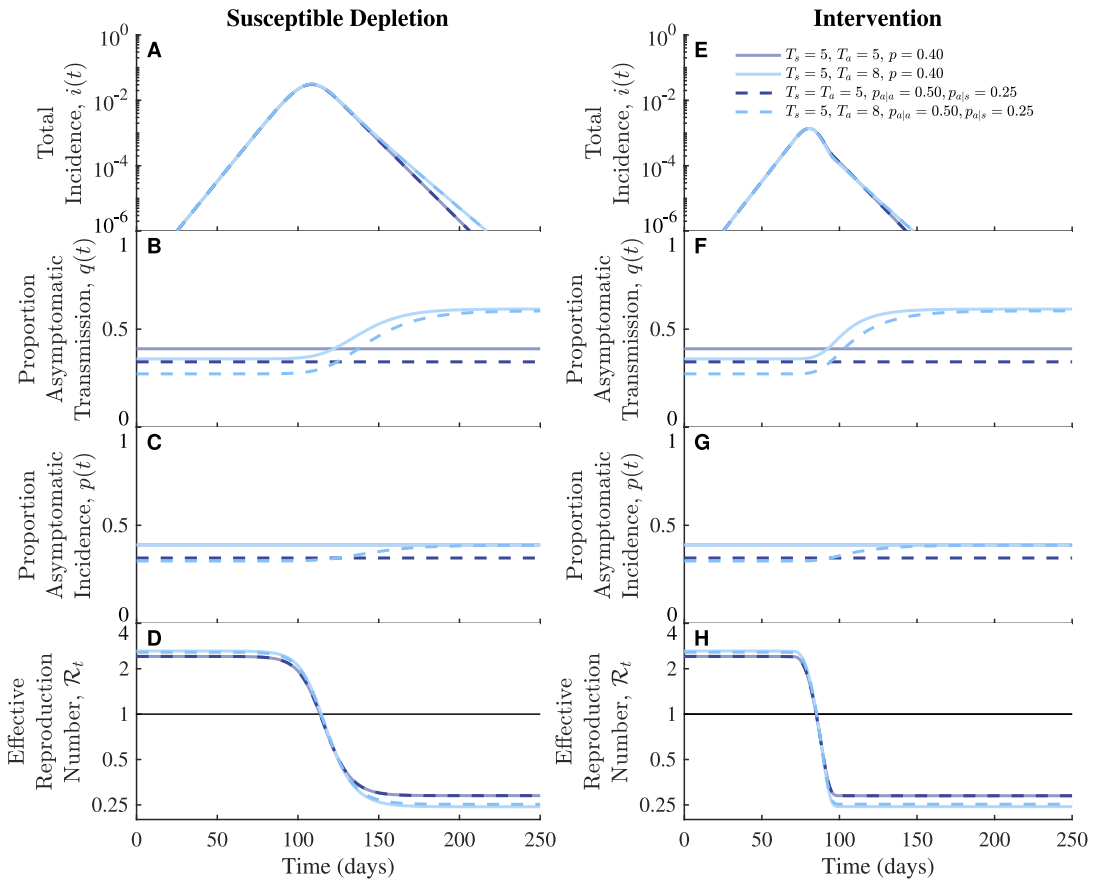

Fig. 2. Effects of transmission correlations and generation-interval differences on the population-level dynamics of asymptomatic infections. We fix the infectious period of symptomatic infections to $T_s = 5$ days and increase the correlation between transmission and disease status. For comparison, we include $T_a = 5$ and $T_a = 8$ days with fixed intrinsic proportion asymptomatic incidence ($p = 0.40$; solid) which are the same as in Fig. 1. When generation intervals are equal, dynamics of incident infections are the same across correlated and uncorrelated cases, but the initial realized proportion of asymptomatic infections are less with correlations (dashed dark blue) than compared to without (solid dark blue). In both the susceptible depletion (A–D) and intervention cases (E–H), longer generation intervals of asymptomatic transmission ($T_a = 8$ days) lead to increases in the realized proportion of asymptomatic transmission over time (B,F, light blue curves). Coupling correlations between transmission and disease statuses with longer generation intervals of asymptomatic transmission cause the realized proportion of asymptomatic incidence to increase over time (C,G, dashed light blue). The exponential growth rate, $r = 0.14$ days^{-1}, is matched across all simulations (Methods). Proportions asymptomatic are $p = 0.40$ (solid lines) and $p_{a|a} = 0.50$, $p_{a|s} = 0.25$ (dashed lines). Parameter values: $\mathcal{R}_0 = 2.41$, $\beta_a = \beta_s = 0.483$ days^{-1} (dashed dark blue); $\mathcal{R}_0 = 2.58$, $\beta_a = 0.322$ days^{-1}, $\beta_s = 0.515$ days^{-1} (dashed light blue).

of asymptomatic transmission and incidence also remain constant over time—in this case, the proportions are lower than the intrinsic proportion asymptomatic incidence ($p = 0.40$) (Fig. 2B,F and C,G; dashed dark blue), because the ratio between the increase in asymptomatic infectees per asymptomatic infector ($p_{a|a} - p$) and the decrease in asymptomatic infectees per symptomatic infector ($p - p_{a|s}$) is less than $(1-p)/p$. When asymptomatic individuals have longer infectious periods (and therefore longer generation intervals), correlations between transmission outcomes and disease statuses exaggerate the effect of differences in the transmission time scale—the initial proportion of asymptomatic infections is lower (Fig. 2C,G; light blue curves) and the realized proportion of asymptomatic transmission increases by a greater amount (Fig. 2B,F; light blue curves). In particular, an increase in asymptomatic transmission also causes the proportion of asymptomatic incidence to increase because transmission from asymptomatically infected individuals are more likely to result in new asymptomatic infections (Fig. 2C,G; dashed light blue).

In addition, the secondary attack rates of symptomatic infections may be greater than asymptomatic infections, as much as four-fold greater (Wu et al., 2020). To examine this upper estimate, we set $p_{a|a} = 0.50$ and $p_{a|s} = 0.25$ and assume $\mathcal{R}_{0,s} = 4\,\mathcal{R}_{0,s}$. We show the effects on proportions of asymptomatic transmission and incidence over the range of infectious-period ratios: $T_a/T_s = [5/8, 8/5]$. The difference between the intrinsic and realized proportions of asymptomatic transmission decreases with increasing ratio of T_a/T_s, passing through zero when $T_a/T_s = 1$ (Figure S7A). The realized proportion of asymptomatic transmission increases over time for $T_a/T_s > 1$, remains constant for $T_a/T_s = 1$, and decreases over time for $T_a/T_s < 1$. (Figure S7B). The changes when $\mathcal{R}_{0,s} = 4\,\mathcal{R}_{0,a}$ (gray) are less pronounced than when $\mathcal{R}_{0,s} = \mathcal{R}_{0,a}$ (black). In both cases, the changes are larger with correlations $p_{a|a} = 0.5$ and $p_{a|s} = 0.25$ (dashed) than without (solid), consistent with the effects shown in Fig. 2B,F, and with correlations, the realized proportion of asymptomatic incidence during exponential growth, $p(0)$, is less than the value of the intrinsic proportion, $p = 0.4$ (Figure S7C). In addition, the realized proportion of asymptomatic incidence increases over time for $T_a/T_s > 1$, remains constant for $T_a/T_s = 1$, and decreases over time for $T_a/T_s < 1$ (Figure S7D). The changes are less pronounced when $\mathcal{R}_{0,s} = 4\,\mathcal{R}_{0,a}$ than when $\mathcal{R}_{0,s} = \mathcal{R}_{0,a}$.

3.3. Effects of age-dependent mixing

Finally, we consider the effects of coupling age-dependent assortativity and symptomaticity as an example of how correlations might arise between transmission outcomes and disease statuses. Since symptomaticity is correlated with age, and since individuals are more likely to mix with other individuals of similar age groups, relatively higher proportions of asymptomatic (symptomatic) secondary infections are due to transmission from asymptomatic (symptomatic) primary infections. To investigate the effect of age-dependent heterogeneity on

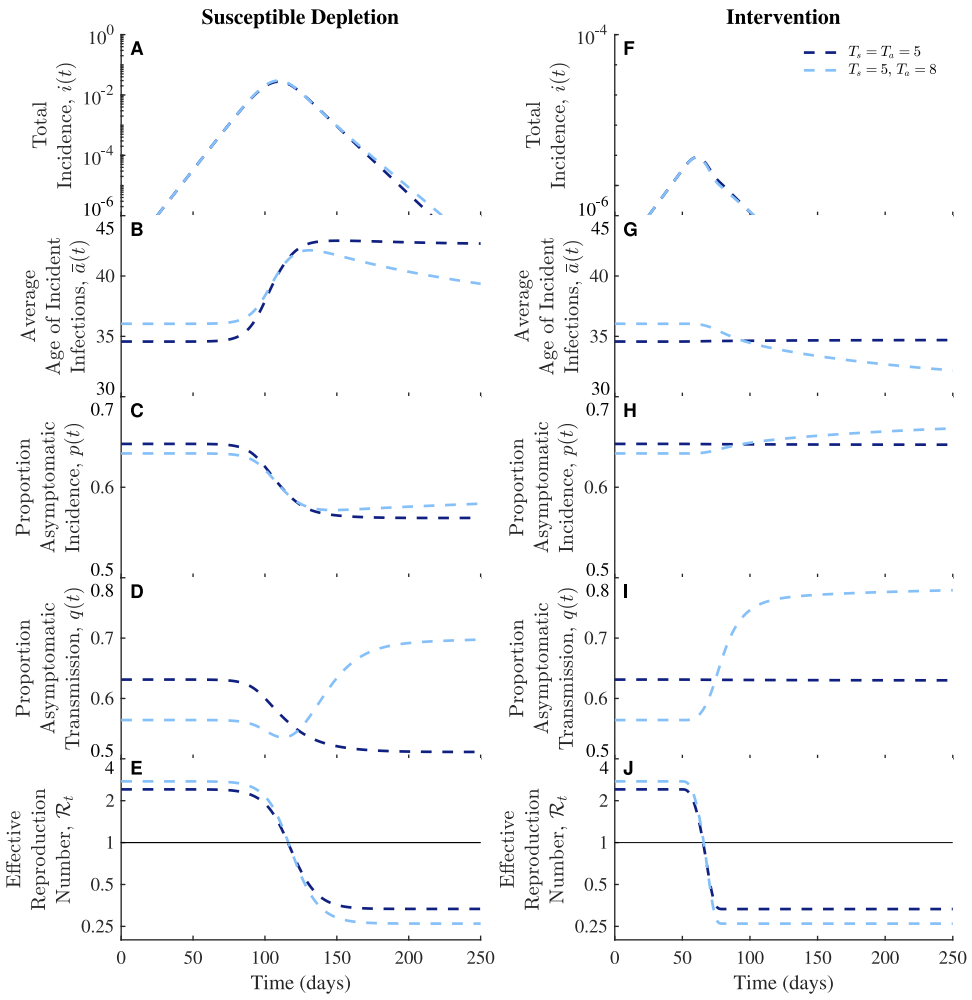

Fig. 3. Effects of age-dependent mixing and generation-interval differences on the population-level dynamics of asymptomatic infections. We fix the symptomatic infectious period to $T_s = 5$ days and compare when the asymptomatic infectious period is equal to ($T_a = T_s = 5$ days; dark blue) or longer than the symptomatic infectious period ($T_a = 8$ days; light blue). We show susceptible depletion (A–E) and intervention scenarios (F–J). As the average age of an incident infection changes over time (C,H), so do the realized proportions of asymptomatic incidence (C,H) and transmission (D,I). Across all simulations, the intrinsic proportion of asymptomatic incidence is 0.648, and the exponential growth rate is $r = 0.14$ days^{-1} (Methods). Other parameter values: $\mathcal{R}_0 = 2.41$ (dark blue); $\mathcal{R}_0 = 2.75$ (light blue).

the dynamics of asymptomatic infections, we parametrize an age-dependent SEIR model by allowing the contact rates and the proportions of asymptomatic incidence to vary across age groups (Methods).

First, we consider age-dependent assortative mixing in contacts and examine the effects of introducing age-dependent variation in proportion of asymptomatic infection (Figure S8). In the absence of intervention, the average age of an incident infection increases as the epidemic progresses in this example because higher contact rates of younger individuals drive faster susceptible depletion (Figure S8B). An increase in the mean age of infection translates to a decrease in both the proportion of asymptomatic incidence (Figure S8C) and transmission (Figure S8D). In contrast, intervention prevents significant susceptible depletion of each age group, and thus, the age distribution of incident infections, and therefore proportions of asymptomatic transmission and infections, remains roughly constant over time (Figure S8G–I).

When we increase the mean infectious period of asymptomatic individuals, longer generation intervals from young, asymptomatic individuals become relatively more important during the decay phase; therefore, the mean age of an incident infection decreases (Fig. 3B, G; light blue) and the proportions of asymptomatic transmission and incidence increase (Fig. 3C, D, H, I; light blue). In this example, we assume equal reproduction numbers between symptomatic and asymptomatic individuals. For comparison, we also consider differences in generation intervals when symptomatic and asymptomatic transmission rates are assumed equal (Figure S9). Overall, we find that the two formulations show similar qualitative trends but differ quantitatively: for a longer asymptomatic infectious period, the initial average age of incident infections is lower than when symptomatic and asymptomatic reproduction numbers are equal. As a result, when the susceptible population is depleted, the effects of age-dependent heterogeneity lead to larger increases in the average age of incident infections as the epidemic grows. Moreover, when intervention is applied, these effects lead to smaller decreases in the average age of incident infections during the decay phase compared to when the reproduction numbers are equal (compare light blue curves in Fig. 3B vs. Figure S9B).

4. Discussion

Using a series of nonlinear epidemice models, we found that time-scale differences in transmission dynamics between symptomatic and asymptomatic individuals can shape population-level epidemic dynamics. In particular, when asymptomatic individuals transmit for longer, the proportion of asymptomatic transmission tends to increase as the epidemic decays because longer generation intervals of asymptomatic transmission become more important; this result generalizes earlier work, which illustrated the same effect for the initial exponential growth phase (Park et al., 2020). Further accounting for the possibility

that asymptomatic individuals are more likely to generate asymptomatic infections can amplify this effect, and also increase the proportion of asymptomatic *incidence*. Our findings suggest that neglecting differences in the time profile of transmission between symptomatic and asymptomatic individuals can systematically bias estimates of disease severity, not only during the initial growth phase (Park et al., 2020) but also over the course of the epidemic. These results indicate that the intensity of the disease burden may vary over the course of an outbreak, with a potentially higher proportion of undetected infections as the incidence decreases. Hence, increasing asymptomatic surveillance as an outbreak wanes may help prevent subsequent epidemic waves.

We extended the model framework to include the effects of age-dependent heterogeneity in disease severity and assortativity in mixing patterns. When the disease is allowed to spread unchecked, the effects of susceptible depletion dominates the dynamics, resulting in an increase in the mean age of infection through time. However, when we account for the possibility that the asymptomatic individual infections may be longer, the proportion of new infections attributable to transmission from younger individuals increases during the decay phase, tending to decrease the mean age of infection; if asymptomatic infections are long and the epidemic is controlled by intervention or behavior change, the mean age of infection can be lower in the declining than in the increasing phase. Notably, the age distribution of SARS-CoV-2 infections changed in the US and UK during summer 2020 (Boehmer et al., 2020; Riley et al., 2021). For example, the median age of cases decreased from a range of 45–50 years of age to a range of 33–37 years from May to June as the number of cases decreased across all four US census regions (Boehmer et al. (2020), Figure S10 in Supplementary material). Previous studies primarily attributed these changes to behavioral effects; however, our analysis shows that individual-level differences in transmission dynamics of asymptomatic and symptomatic individuals could have also contributed to these changes. Our results indicate that with longer time scales of asymptomatic transmission, the distribution of infections will tend toward younger individuals as the epidemic declines. Hence, controlling asymptomatic spread may be especially relevant as incidence declines, which, in this scenario, means that it may make sense to shift attention towards younger age groups (e.g., with asymptomatic surveillance or school-based interventions).

Our study comes with a number of caveats. First, we assumed that the asymptomatic individuals transmit longer than symptomatic individuals. However, the opposite can be also true: asymptomatic individuals may recover faster and therefore have shorter infectious periods. The consequences of this assumption (i.e., faster asymptomatic transmission) are straightforward to predict: shorter asymptomatic generation intervals become more important during the growth phase, which in turn can increase the initial proportion of asymptomatic incidence and transmission. Second, throughout we considered an idealized intervention which reduces transmission rate by a fixed amount, but real interventions will be more complex. Some interventions, such as contact tracing and self-isolation, are more likely to reduce late transmission by symptomatic individuals and therefore lead to bigger differences between symptomatic and asymptomatic individuals. Other interventions, such as frequent mass testing, will have similar effects on symptomatic and asymptomatic individuals by an equal amount but may still have qualitatively different effects from the intervention we considered (which assumes generation interval distributions are not affected by intervention). Nonetheless, major interventions that drove the current pandemic (e.g., social distancing, mask wearing, and vaccination) are expected to be similar to the idealized intervention we considered. As a result, we expect our qualitative result to be broadly applicable in scenarios where asymptomatic individuals transmit for a longer amount of time. Despite these limitations, our study highlights the importance of characterizing the differences in transmission time scale in understanding epidemic dynamics.

We emphasize that virus-driven correlations (i.e., asymptomatic transmission is more likely to result in asymptomatic infection) are distinct from demographic correlations (i.e., younger individuals are more likely to infect younger individuals due to assortative mixing). We considered these two correlations separately for simplicity, but both correlations may be present in an actual epidemic: that is, young individuals infected by young asymptomatic infectors may be more likely to remain asymptomatic than those infected by young symptomatic infectors. Coupling of both correlations may further amplify changes in the amount of asymptomatic transmission and incidence over the course of an epidemic.

The dynamics of asymptomatic transmission remain uncertain, despite SARS-CoV-2 having spread throughout the world for over 2 years. More work is needed to better characterize the course of asymptomatic infections with respect to both transmission potential and the duration of infection. Accounting for these sources of individual variation along with the effects of mitigation may aid in understanding how the relative contribution of asymptomatic infections shape epidemic dynamics and in improving the development and deployment of effective control measures.

Declaration of competing interest

The authors declare that they have no known competing financial interests or personal relationships that could have appeared to influence the work reported in this paper.

Data availability

The codes and data are available for download at: https://doi.org/10.5281/zenodo.7523452.

Acknowledgments

The authors thank Guanlin Li for contributions to early model development incorporating correlations and David Demory for code review.

Funding

This work was supported in part by a grant from the Simons Foundation, United States (722153) and support from the Charities in Aid Foundation, the Marier Cunningham Foundation, and the Chaires Blaise Pascal program of the Île-de-France region.

Supplementary material

Supplementary material related to this article can be found online at https://doi.org/10.1016/j.epidem.2022.100664.

References

Anderson, R.M., May, R.M., 1992. Infectious Diseases of Humans: Dynamics and Control. Oxford University Press.

Bai, Y., Yao, L., Wei, T., Tian, F., Jin, D.-Y., Chen, L., Wang, M., 2020. Presumed asymptomatic carrier transmission of COVID-19. JAMA 323 (14), 1406–1407.

Boehmer, T.K., DeVies, J., Caruso, E., van Santen, K.L., Tang, S., Black, C.L., Hartnett, K.P., Kite-Powell, A., Dietz, S., Lozier, M., et al., 2020. Changing age distribution of the COVID-19 pandemic—United States, May–August 2020. Morb. Mortal. Wkly. Rep. 69 (39), 1404.

Brett, T.S., Rohani, P., 2020. Transmission dynamics reveal the impracticality of COVID-19 herd immunity strategies. Proc. Natl. Acad. Sci. 117 (41), 25897–25903.

Buitrago-Garcia, D., Egli-Gany, D., Counotte, M.J., Hossmann, S., Imeri, H., Ipekci, A.M., Salanti, G., Low, N., 2020. Occurrence and transmission potential of asymptomatic and presymptomatic SARS-CoV-2 infections: A living systematic review and meta-analysis. PLoS Med. 17 (9), e1003346.

Byrne, A.W., McEvoy, D., Collins, A.B., Hunt, K., Casey, M., Barber, A., Butler, F., Griffin, J., Lane, E.A., McAloon, C., et al., 2020. Inferred duration of infectious period of SARS-CoV-2: rapid scoping review and analysis of available evidence for asymptomatic and symptomatic COVID-19 cases. BMJ Open 10 (8), e039856.

Champredon, D., Dushoff, J., 2015. Intrinsic and realized generation intervals in infectious-disease transmission. Proc. R. Soc. B 282 (1821), 20152026.
Chan, J.F.W., Yuan, S., Kok, K.-H., To, K.K.-W., Chu, H., Yang, J., Xing, F., Liu, J., Yip, C.C.-Y., Poon, R.W.-S., et al., 2020. A familial cluster of pneumonia associated with the 2019 novel Coronavirus indicating person-to-person transmission: a study of a family cluster. Lancet 395 (10223), 514–523.
Chinazzi, M., Davis, J.T., Ajelli, M., Gioannini, C., Litvinova, M., Merler, S., y Piontti, A.P., Mu, K., Rossi, L., Sun, K., et al., 2020. The effect of travel restrictions on the spread of the 2019 novel coronavirus (COVID-19) outbreak. Science 368 (6489), 395–400.
Davies, N.G., Klepac, P., Liu, Y., Prem, K., Jit, M., Eggo, R.M., 2020. Age-dependent effects in the transmission and control of COVID-19 epidemics. Nat. Med. 26 (8), 1205–1211.
Diekmann, O., Heesterbeek, J.A.P., 2000. Mathematical Epidemiology of Infectious Diseases: Model Building, Analysis and Interpretation, Vol. 5. John Wiley & Sons.
Diekmann, O., Heesterbeek, J.A.P., Metz, J.A., 1990. On the definition and the computation of the basic reproduction ratio R0 in models for infectious diseases in heterogeneous populations. J. Math. Biol. 28 (4), 365–382.
Ferretti, L., Wymant, C., Kendall, M., Zhao, L., Nurtay, A., Abeler-Dörner, L., Parker, M., Bonsall, D., Fraser, C., 2020. Quantifying SARS-CoV-2 transmission suggests epidemic control with digital contact tracing. Science 368 (6491).
Fraser, C., Riley, S., Anderson, R.M., Ferguson, N.M., 2004. Factors that make an infectious disease outbreak controllable. Proc. Natl. Acad. Sci. 101 (16), 6146–6151.
He, X., Lau, E.H., Wu, P., Deng, X., Wang, J., Hao, X., Lau, Y.C., Wong, J.Y., Guan, Y., Tan, X., et al., 2020. Temporal dynamics in viral shedding and transmissibility of COVID-19. Nat. Med. 26 (5), 672–675.
Heesterbeek, J., Dietz, K., 1996. The concept of R0 in epidemic theory. Stat. Neerl. 50 (1), 89–110.
Imai, M., Iwatsuki-Horimoto, K., Hatta, M., Loeber, S., Halfmann, P.J., Nakajima, N., Watanabe, T., Ujie, M., Takahashi, K., Ito, M., et al., 2020. Syrian hamsters as a small animal model for SARS-CoV-2 infection and countermeasure development. Proc. Natl. Acad. Sci. 117 (28), 16587–16595.
Johansson, M.A., Quandelacy, T.M., Kada, S., Prasad, P.V., Steele, M., Brooks, J.T., Slayton, R.B., Biggerstaff, M., Butler, J.C., 2021. SARS-CoV-2 transmission from people without COVID-19 symptoms. JAMA Netw. Open 4 (1), e2035057.
Jones, T.C., Biele, G., Mühlemann, B., Veith, T., Schneider, J., Beheim-Schwarzbach, J., Bleicker, T., Tesch, J., Schmidt, M.L., Sander, L.E., et al., 2021. Estimating infectiousness throughout SARS-CoV-2 infection course. Science 373 (6551), eabi5273.
Ke, R., Zitzmann, C., Ribeiro, R.M., Perelson, A.S., 2020. Kinetics of SARS-CoV-2 infection in the human upper and lower respiratory tracts and their relationship with infectiousness. MedRxiv.
Kinoshita, R., Anzai, A., Jung, S.-m., Linton, N.M., Miyama, T., Kobayashi, T., Hayashi, K., Suzuki, A., Yang, Y., Akhmetzhanov, A.R., et al., 2020. Containment, contact tracing and asymptomatic transmission of novel Coronavirus disease (COVID-19): a modelling study. J. Clin. Med. 9 (10), 3125.
Lavezzo, E., Franchin, E., Ciavarella, C., Cuomo-Dannenburg, G., Barzon, L., Del Vecchio, C., Rossi, L., Manganelli, R., Loregian, A., Navarin, N., et al., 2020. Suppression of a SARS-CoV-2 outbreak in the Italian municipality of Vo'. Nature 584 (7821), 425–429.
Lee, S., Kim, T., Lee, E., Lee, C., Kim, H., Rhee, H., Park, S.Y., Son, H., Yu, S., Park, J.W., et al., 2020. Clinical course and molecular viral shedding among asymptomatic and symptomatic patients with SARS-CoV-2 infection in a community treatment center in the Republic of Korea. JAMA Int. Med. 180 (11), 1447–1452.
Li, R., Pei, S., Chen, B., Song, Y., Zhang, T., Yang, W., Shaman, J., 2020. Substantial undocumented infection facilitates the rapid dissemination of novel coronavirus (SARS-CoV-2). Science 368 (6490), 489–493.
Long, Q.-X., Tang, X.-J., Shi, Q.-L., Li, Q., Deng, H.-J., Yuan, J., Hu, J.-L., Xu, W., Zhang, Y., Lv, F.-J., et al., 2020. Clinical and immunological assessment of asymptomatic SARS-CoV-2 infections. Nat. Med. 26 (8), 1200–1204.
Marks, M., Millat-Martinez, P., Ouchi, D., h Roberts, C., Alemany, A., Corbacho-Monné, M., Ubals, M., Tobias, A., Tebé, C., Ballana, E., et al., 2021. Transmission of COVID-19 in 282 clusters in Catalonia, Spain: a cohort study. Lancet Infect. Dis. 21 (5), 629–636.
Mizumoto, K., Kagaya, K., Zarebski, A., Chowell, G., 2020. Estimating the asymptomatic proportion of Coronavirus disease 2019 (COVID-19) cases on board the Diamond Princess cruise ship, Yokohama, Japan, 2020. Eurosurveillance 25 (10), 2000180.
Nishiura, H., Kobayashi, T., Miyama, T., Suzuki, A., Jung, S.-m., Hayashi, K., Kinoshita, R., Yang, Y., Yuan, B., Akhmetzhanov, A.R., et al., 2020. Estimation of the asymptomatic ratio of novel Coronavirus infections (COVID-19). Int. J. Infect. Dis. 94, 154.
Oran, D.P., Topol, E.J., 2020. Prevalence of asymptomatic SARS-CoV-2 infection: a narrative review. Ann. Int. Med. 173 (5), 362–367.
Pan, X., Chen, D., Xia, Y., Wu, X., Li, T., Ou, X., Zhou, L., Liu, J., 2020. Asymptomatic cases in a family cluster with SARS-CoV-2 infection. Lancet Infect. Dis. 20 (4), 410–411.
Park, S.W., Champredon, D., Weitz, J.S., Dushoff, J., 2019. A practical generation-interval-based approach to inferring the strength of epidemics from their speed. Epidemics 27, 12–18.
Park, S.W., Cornforth, D.M., Dushoff, J., Weitz, J.S., 2020. The time scale of asymptomatic transmission affects estimates of epidemic potential in the COVID-19 outbreak. Epidemics 31, 100392.
Riley, S., Ainslie, K.E., Eales, O., Walters, C.E., Wang, H., Atchison, C., Fronterre, C., Diggle, P.J., Ashby, D., Donnelly, C.A., et al., 2021. Resurgence of SARS-CoV-2: detection by community viral surveillance. Science.
Roberts, M., Heesterbeek, J., 2007. Model-consistent estimation of the basic reproduction number from the incidence of an emerging infection. J. Math. Biol. 55 (5), 803–816.
Russell, T.W., Hellewell, J., Jarvis, C.I., Van Zandvoort, K., Abbott, S., Ratnayake, R., Flasche, S., Eggo, R.M., Edmunds, W.J., Kucharski, A.J., et al., 2020. Estimating the infection and case fatality ratio for coronavirus disease (COVID-19) using age-adjusted data from the outbreak on the diamond Princess cruise ship, February 2020. Eurosurveillance 25 (12), 2000256.
Ryan, K.A., Bewley, K.R., Fotheringham, S.A., Slack, G.S., Brown, P., Hall, Y., Wand, N.I., Marriott, A.C., Cavell, B.E., Tree, J.A., et al., 2021. Dose-dependent response to infection with SARS-CoV-2 in the ferret model and evidence of protective immunity. Nature Commun. 12 (1), 1–13.
Svensson, A., 2007. A note on generation times in epidemic models. Math. Biosci. 208 (1), 300–311.
Van den Driessche, P., Watmough, J., 2002. Reproduction numbers and sub-threshold endemic equilibria for compartmental models of disease transmission. Math. Biosci. 180 (1–2), 29–48.
Wallinga, J., Lipsitch, M., 2007. How generation intervals shape the relationship between growth rates and reproductive numbers. Proc. R. Soc. B 274 (1609), 599–604.
Wallinga, J., Teunis, P., 2004. Different epidemic curves for severe acute respiratory syndrome reveal similar impacts of control measures. Am. J. Epidemiol. 160 (6), 509–516.
Watanabe, T., Bartrand, T.A., Weir, M.H., Omura, T., Haas, C.N., 2010. Development of a dose-response model for SARS coronavirus. Risk Anal.: Int. J. 30 (7), 1129–1138.
Wu, J.T., Leung, K., Bushman, M., Kishore, N., Niehus, R., de Salazar, P.M., Cowling, B.J., Lipsitch, M., Leung, G.M., 2020. Estimating clinical severity of COVID-19 from the transmission dynamics in Wuhan, China. Nat. Med. 26 (4), 506–510.
Zhang, J., Litvinova, M., Liang, Y., Wang, Y., Wang, W., Zhao, S., Wu, Q., Merler, S., Viboud, C., Vespignani, A., et al., 2020. Changes in contact patterns shape the dynamics of the COVID-19 outbreak in China. Science 368 (6498), 1481–1486.
Zheng, S., Fan, J., Yu, F., Feng, B., Lou, B., Zou, Q., Xie, G., Lin, S., Wang, R., Yang, X., et al., 2020. Viral load dynamics and disease severity in patients infected with SARS-CoV-2 in Zhejiang province, China, January-March 2020: retrospective cohort study. Bmj 369.